Biosensors and Bioelectronics 80 (2016) 477–482

Contents lists available at ScienceDirect

Biosensors and Bioelectronics

journal homepage: www.elsevier.com/locate/bios

Quantum dot monolayer for surface plasmon resonance signal enhancement and DNA hybridization detection

Aditya Sharma Ghrera [a], Manoj Kumar Pandey [b], Bansi Dhar Malhotra [b,c,*]

[a] The Northcap University (Formerly ITM University), Gurgaon 122017, India
[b] The DST Centre on Biomolecular Electronics, CSIR-National Physical Laboratory, Dr K S Krishnan Marg, New Delhi 110012, India
[c] Department of Biotechnology, Delhi Technological University, Delhi 110042, India

ARTICLE INFO

Article history:
Received 11 December 2015
Received in revised form
27 January 2016
Accepted 5 February 2016
Available online 6 February 2016

Keywords:
Quantum dots
Cadmium selenide
Surface plasmon resonance
Langmuir–Blodgett
Nucleic acid hybridization
Chronic myelogenous leukemia
Biosensor

ABSTRACT

We report results of studies relating to the fabrication of a surface plasmon resonance (SPR)-based nucleic acid sensor for quantification of DNA sequence specific to chronic myelogeneous leukemia (CML). The SPR disk surface has been modified with octadecanethiol self-assembled monolayer followed by deposition of the tri-n-octylphosphine oxide capped cadmium selenide quantum dots (QD) Langmuir monolayer. The deposition is performed *via* Langmuir–Blodgett (LB) technique. For the sensor chip preparation, covalent immobilization of the thiol-terminated DNA probe sequence (pDNA) using displacement reaction is accomplished. This integrated SPR chip has been used to detect target complementary DNA concentration by monitoring the change in coupling angle *via* hybridization. It is revealed that this biosensor exhibits high sensitivity ($0.7859\ m^0\ pM^{-1}$) towards complementary DNA and can be used to detect it in the concentration range, 180 pM to 5 pM with detection limit as 4.21 pM. The results of kinetic studies yield the values of hybridization and dissociation rate constants as $9.6 \times 10^4\ M^{-1}\ s^{-1}$ and $2.3 \times 10^{-2}\ s^{-1}$, respectively, with the equilibrium constant for hybridization as $4.2 \times 10^6\ M^{-1}$.

1. Introduction

Chronic myelogenous leukemia (CML) occurs in blood-forming cells of the bone marrow and is characterized by specific reciprocal translocation of chromosomes 9 and 22 (Nowell, 2007), producing BCR-ABL oncogene in the abnormal chromosome 22 (Druker et al., 2001). As BCR-ABL oncogene is tumor-specific, detection of this gene may help in the diagnosis of CML and in monitoring of the patients after bone marrow transplantation. Currently, CML diagnosis is performed *via* fluorescence *in situ* hybridization, flow cytometry and real-time quantitative reverse transcription polymerase chain reaction (Lee et al., 2002; Saglio and Fava, 2012). Since all these techniques are laboratory based, they require skilled clinicians and are time-consuming thereby causing delay in the therapeutic treatment. Also, the testing of the patient sample cannot be done on a regular basis. To obtain improved monitoring efficacy, there is increased interest towards the development of sensitive and miniaturized biosensors to enable the point of care diagnostics and monitoring of the disease.

For fabrication of highly sensitive biosensors that can be used for on-line monitoring of biomolecular recoginition event, surface plasmon resonance (SPR) technique has recently gained much attention (Nawattanapaiboon et al., 2015; Tahmasebpour et al., 2015; Xiang et al., 2015). Not only does it offer real-time *in situ* analysis of dynamic surface events, but it may also be used to determine rates of adsorption and desorption for a range of surface interactions. SPR sensor excites the metal/dielectric interface *via* mono- or polychromatic polarized light and generates propagating plasmonic waves. These palsmonic waves are highly sensitive to the refractive index (RI) changes in the sample, which can be directly correlated with the mass density changes on a metal surface, and can be used to measure real-time biomolecular interactions and target quantification. In case of the DNA biosensor, the SPR signal is produced by measuring the RI changes induced by hybridization event. SPR based detection of DNA hybridization has attracted much attention due to applications in medical diagnostics (Cennamo et al., 2015; Singh et al., 2014), biotechnology and life-science research (Huang et al., 2015), agro-food sector (Piliarik et al., 2009; Tran et al., 2013), security and environmental monitoring (Šípová and Homola, 2013).

The SPR is not limited to metals but can also be achieved in semiconductor nanocrystals with appreciable free carrier concentrations. The SPR signal enhancement of Au film has been

* Corresponding author.
E-mail address: bansi.malhotra@gmail.com (B.D. Malhotra).

http://dx.doi.org/10.1016/j.bios.2016.02.013
0956-5663/

reported by the electronic coupling of its surface plasmon wave with the localized plasmon of QD. Zayats et al. have employed this QD-modified Au-disk for the detection of acetylcholine esterase using SPR spectroscopy (Zayats et al., 2003). Hoa et al. have reported that patterned immobilization of QD enhances SPR signal (Hoa et al., 2007). These researchers have demonstrated that patterned immobilization of surface receptor probes, enhanced with the attachment of QD onto zero-order lamellar grating, leads to significant enhancement of the detection threshold of the SPR biosensor. Qi et al. have demonstrated a layer-by layer surface decoration of QD on Au substrate and investigated the interactions between the QD and different proteins using *in situ* SPR technique (Qi et al., 2009). It has been revealed that QD can be used to enhance the SPR signal resulting in higher sensitivity and selectivity for detection of desired biomolecules. Ali et al. have recently reported application of the protein-conjugated QD interface to investigate the binding kinetics using antigen – antibody interaction (Ali et al., 2014) and compared the immunosensing results obtained *via* electrochemical and SPR techniques.

The ordered arrangement of QD with controlled thickness and interparticle spacing can be obtained through the Langmuir–Blodgett (LB) technique. We have recently reported optimized experimental conditions to obtain the stable Langmuir monolayer of CdSe QD and their LB deposition in the form of thin film (Sharma et al., 2012). These thin films are now explored for the fabrication of an SPR based nucleic acid sensor by covalent immobilization of the CML specific thiol terminated DNA as the capture probe. The change in RI value of the sensor on interaction of DNA probe with complementary target sequence identified from BCR-ABL fusion gene, single-base mismatch and non-complementary sequence has been monitored. Besides this, efforts have been made to investigate the kinetics of DNA hybridization at the sensor surface. The SPR response of this biosensor exhibits highly specific interaction with the complementary target DNA with hybridization constant of $9.6 \times 10^4\ M^{-1}\ s^{-1}$ and dissociation constant of $2.3 \times 10^{-2}\ s^{-1}$. To the best of our knowledge the present work is the first report on application of QD-monolayer for SPR-based detection of DNA hybridization.

2. Materials and methods

2.1. Biochemicals and reagents

All the reagents and solvents were of analytical grade and were obtained from Sigma-Aldrich, India. Buffer solutions were prepared in deionized water (Millipore, 18.0 MΩ cm) and were autoclaved prior to being used. CML specific probe oligonucleotide sequence (22 bases) identified from the BCR-ABL gene, complementary, non-complementary and one-base mismatch target sequence, were procured from Sigma-Aldrich, Milwaukee, USA. This probe corresponds specifically to the P210 kDa of BCR-ABL tyrosine kinase fusion product obtained from the reciprocal translocation of 9; 22 (Philidelphia chromosome). DNA sequences that were used for the studies are listed below.

Probe DNA: Thiol-5′-TGTCCACAGCATTCCGCTGACC-3′ (pDNA).
Complementary:5′-GGTCAGCGGAATGCTGTGGACA-3′.
One-base mismatch:5′-G**C**TCAGCGGAATGCTGTGGACA-3′.
Non-complementary:5′-TACTCGCAATAACGTGATCTCC-3′.

All oligonucleotides solutions were prepared in TE buffer (1 M Tris–HCl, 0.5 M EDTA, pH 8.0) and stored at −20 °C.

2.2. Characterization

Monolayer depositions were conducted using an LB trough (NIMA, UK; Model 601A). The surface chemistry measurements at the air–water interface were conducted on an LB trough having dimensions of 10 cm × 30 cm. The computer controlled symmetrically movable barrier was employed to regulate the surface area and constant temperature was maintained using a temperature controller (Julabo F5). The deionized water was used as the monolayer subphase and the surface pressure was measured by the immersed Wilhelmy plate. Fourier transform infrared (FT-IR) measurements were conducted in the ATR mode, with germanium waveguide, using a Perkin-Elmer Spectrum BX II spectrophotometer. The FTIR signal was obtained by averaging 64 scans at the resolution of $4\ cm^{-1}$. The morphological characterization was carried out using scanning electron microscope (SEM, LEO 440). The immobilization and hybridization experiments using SPR studies were recorded using an Autolab SPR, Eco Chemie (Netherlands), based on Kretschmann configuration. In the SPR experiments, linearly p-polarized light from a laser (670 nm) was directed through a prism onto the Au substrate, and the intensity of reflected light as a function of time was measured over a range of 4000 millidegrees (m^0) at 25 °C. In the experiments, an Au-coated glass substrate was coupled with the plane face of the prism *via* an index matching fluid.

2.3. Synthesis of CdSe quantum dots

TOPO-capped CdSe nanocrystals were synthesized according to the modified Peng and Peng's method (Peng and Peng, 2000). For the preparation of trioctylphosphine selenide (TOPSe) solution, selenium powder (0.175 g) was dissolved in TOP (3 ml) and stirred for 24 h. In another reaction, cadmium oxide(CdO; 0.220 g), hexyl phosphonic acid (0.122 g) and tri-n-octylphosphine oxide (TOPO; 1.843 g) were mixed in a two-necked flask and heated to 320 °C under argon atmosphere, until CdO powder was completely dissolved in the solution (Foos et al. 2006). After 6 h, the solution was cooled down to 250 °C, and TOPSe solution was injected rapidly into the flask. The solution was further cooled down to 50 °C, and methanol (10 ml) was added for precipitation of the CdSe nanocrystals. Thus obtained CdSe quantum dots were washed several times with methanol to remove excess residues and in the end TOPO-capped CdSe nanocrystal powders were obtained by drying in a vacuum oven.

2.4. Pre-treatment of SPR disk

Prior to their immobilization, SPR disks were treated with piranha solution followed by rinsing with de-ionized water and subsequent ultrasonication in absolute ethanol (for about 2 min) along with consecutive rinsing with de-ionized water. The SPR disk was treated with 1 mM ethanolic solution of 1-octadecanethiol (ODT) for 10 min (Ishida et al., 1997) to render it hydrophobic. The disk was again washed with ethanol to remove un-bound ODT molecules.

2.5. Langmuir–Blodgett deposition of QD monolayer

The details of optimization conditions for the CdSe Langmuir monolayer were presented in a previous report (Sharma et al., 2012). Typically, 40 μL solution of CdSe (3 mg mL^{-1} in chloroform) was vortexed with 20 μL of stearic acid (SA) solution (1 mg mL^{-1} in chloroform) for about 5 min followed by gentle spreading on the water subphase. Incorporation of SA molecules in CdSe-QD not only leads to reduction of the aggregate formation and improvement of its spreading behavior (Cheung and Rubner, 1994) but also prevents inter-digitation of the hydrophobic tails of TOPO molecules, thus acting as a spacer (Sharma et al., 2012). The solution was left for 30 min so that the chloroform could be evaporated. The pre-hydrophobized SPR disk was positioned perpendicular to

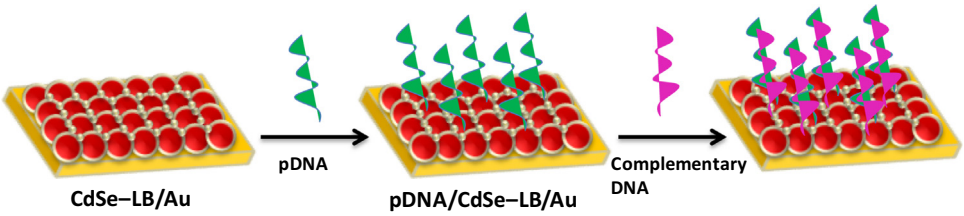

Fig. 1. Schematic showing the steps involved in the fabrication of pDNA/CdSe-LB/Au sensor disk.

air–water interface and the monolayer was subsequently deposited by vertical dipping at a rate of 10 mm min^{-1}. In order to gain insight into the CdSe-QD arrangement over the SPR disk after LB deposition, transmission electron microscopic (TEM) technique was used. Under similar experimental conditions, the QDs were deposited over the 200–mesh carbon coated Cu grid under and TEM analysis of the sample was performed. The TEM image indicates uniformly distributed particulates revealing that the ordered arrangement of CdSe-QD at the air–water interface is preserved at the solid substrate (Fig. S1).

2.6. Immobilization of DNA probe

The probe DNA molecules were immobilized on the surface of CdSe-LB/Au disk (Fig. 1) and the binding was monitored using the SPR technique. The pDNA solution (50 mM), prepared in auto-claved de-ionized water, was allowed to interact with the QD modified disk for 3 h at 25 °C. The thiol terminal of the DNA probe displaced the TOPO molecules over the CdSe surface and allowed their chemisorption over the SPR disk. The pDNA/CdSe-LB/Au disk was repeatedly rinsed with water to remove any unbound pDNA on the substrate surface and the fabricated disk was utilized for CML detection using SPR technique.

2.7. Hybridization studies

For carrying out hybridization studies, the SPR experiment proceeded in triplicate phase format and the corresponding signal was monitored. Initially, before starting the experiment, the SPR signal was recorded with deionized water. The recording was performed for 300 s to obtain the baseline value. In the primary phase, the solution of target sequence was introduced into the channels and was allowed to interact with the sensor surface for the next 1800 s. The hybridization process occurs during this period and the phase is known as association (hybridization) phase. The change in the coupling angle (θ) before and after the hybridization phase corresponds to the amount of binding while keeping all other parameters constant. The next is dissociation phase, which involves the removal of un-hybridized DNA from the sensor surface. For this, the unused solution was discarded and the sensor was washed with de-ionized water through automated process. The final phase involved the regeneration phase, where the hybridized DNA strands were separated and the sensor was made ready for the next hybridization cycle. The regeneration could be achieved either by treating the sensor with strong acid or strong base. Since better regeneration results were obtained in acidic conditions (Prabhakar et al., 2008), we carried out the sensor regeneration with 5.0 mM hydrochloric acid for 120 s.

3. Results and discussion

3.1. Monitoring of probe DNA immobilization

Fig. 2 shows the SPR response before and after LB deposition of

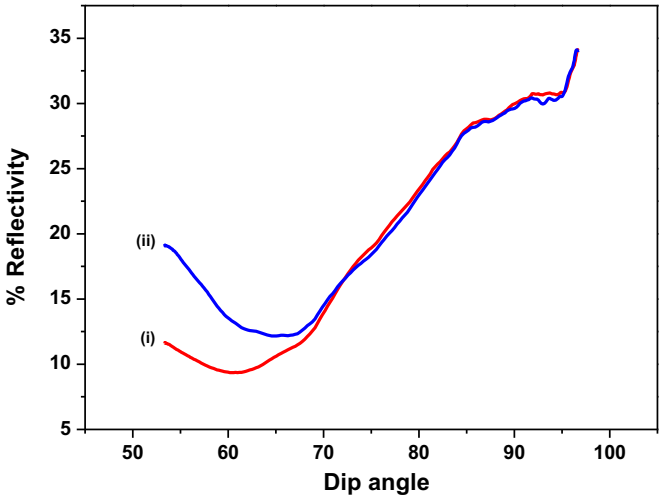

Fig. 2. Surface plasmon resonance curve for (i) the self-assembled monolayer of ODT on a Au film and (ii) same after the deposition of QD monolayer.

QD over the ODT-self assembled monolayer (SAM) modified Au disk. The SPR curve can be seen to shift to the right (increased value) as the QD are deposited at the Au surface. This is in agreement with the results reported in literature (Hoa et al., 2007; Zayats et al., 2003). The sensitivity of the SPR technique lies in the propagation of an evanescent surface plasmon wave at the boundary of metal/medium (dielectric) interface, which may be perturbed due to adsorption of the biomolecules. This is the basis of SPR spectroscopy wherein change in θ can be related to changes in refractive index (*i.e.*, the presence of thin adlayers) at the surface of the metal. Fig. 3 shows SPR sensorgrams obtained for the thiolated DNA immobilization over the surface of SPR disk and QD modified SPR disk. It can be seen that the first phase of 120 s the baseline, after which solution of the thiolated DNA is introduced

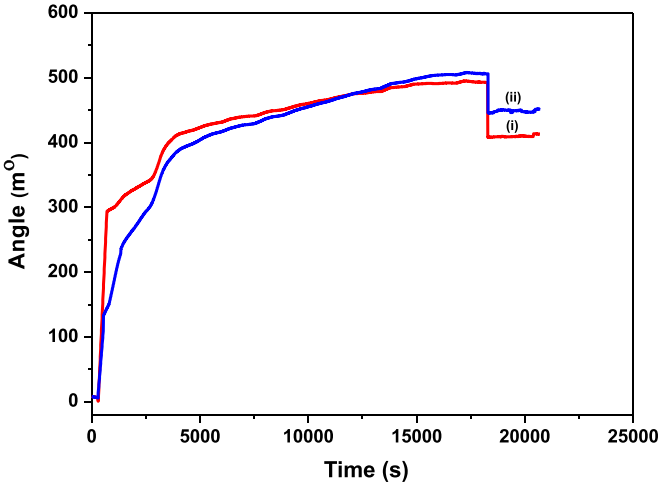

Fig. 3. SPR sensorgrams for covalent immobilization of thiolated DNA probe on the surface of (i) SPR disk and (ii) QD (CdSe-LB) modified SPR disk.

for immobilization for 10,800 s at 25 °C, followed by a washing step. The change in θ corresponds to the amount of binding of DNA at the surface. It has been found that there is a large change in θ (698 m^0) during the initial 3000 s when DNA immobilization is carried out directly at the SPR disk. The change is, however, less for the QD modified disk during this period. This may be because faster immobilization occurs at the Au surface as compared to the CdSe surface. However, pDNA/CdSe-LB/Au disk yields comparable θ value as that for pDNA/Au disk after about 15,000 s.

3.2. Characterization of pDNA/CdSe-LB/au disk

The FT-IR spectrum of pDNA/CdSe-LB/Au disk was recorded and compared with that of CdSe-LB/Au disk to confirm the pDNA immobilization (Fig. S2). The FT-IR spectrum of CdSe-LB/Au disk (Fig. S2, curve i) displays peaks at 2954 cm^{-1}, 2910 cm^{-1}, and 2844 cm^{-1} that can be assigned to C–H stretching of the octyl chains present in TOPO and octadecyl chain in the ODT moiety, and a broad band in the range of 1420–1210 cm^{-1} exhibits peaks corresponding to P=O and C–O stretching (von Holt et al., 2008). Further, a low intensity peak at about 1725 cm^{-1} corresponding to carbonyl stretching vibrational mode of SA molecules is observed and this peak gets intense after immobilization of pDNA (Fig. S2, curve ii). The peaks seen at 1606 cm^{-1} and 1448 cm^{-1} in pDNA/CdSe-LB/Au disk are assigned to –NH bending and –CN stretching, respectively, and can be correlated with the presence of nucleoside bases (Prabhakar et al., 2011; Sharma et al., 2012). Additionally, the peaks found at 674 cm^{-1} arising due to –CS stretching and 1086 cm^{-1} correspond to phosphate stretching indicating successful immobilization of oligonucleotide molecules over the CdSe-LB/Au disk.

The morphological changes at the SPR disk, arising as a result of surface modification, were examined using scanning electron microscopic technique and results are displayed in Fig. S3. As can be seen (Fig. S3, panel i), the ODT-SAM on the Au surface makes it slightly rough. After LB deposition, a uniform distribution of the QD over the surface of Au-substrate can be seen (Fig. S3, panel ii). A regularly arranged globular structure in the micron scale indicates that ordered arrangement of the quantum dots onto the transducer surface provides a favorable environment for immobilization of pDNA in an oriented manner. When CdSe-LB/Au disk is incubated with pDNA, the spherical shape is found to be diminished (Fig. S3, panel iii). This change in morphology is due to the immobilization of pDNA over the QD surface.

3.3. Hybridization detection using SPR technique

Fig. 4 shows results of the SPR studies of pDNA/CdSe-LB/Au disk as a function of time for different concentrations of complementary target DNA sequence. In the SPR signal of pDNA/CdSe-LB/Au disk, 170 m^0 change in θ is seen after incubation with the complementary target (180 pM) for 1800 s, indicating hybridization of the immobilized pDNA with complementary DNA sequence (Fig. 4, Curve i). The change in θ is found to be less as the complementary DNA concentration is decreased (Fig. 4, Curve ii–vi). Fig. S4 shows variation in θ as a function of complementary DNA concentration. It is found that θ of pDNA/CdSe-LB/Au disk decreases linearly with decrease in complementary DNA concentration in the range from 180 pM to 5 pM. The sensitivity of the pDNA/CdSe-LB/Au biosensor has been calculated to be as 0.7859 m^0 pM^{-1} from the calibration curve with a lower detection limit of 4.21 pM (3*SD/sensitivity).

Fig. 5 presents SPR curves obtained for the pDNA/CdSe-LB/Au after hybridization with the complementary, one-base mismatch and non-complementary sequences, respectively. As mentioned earlier, the change in θ of 170 m^0 is observed with the

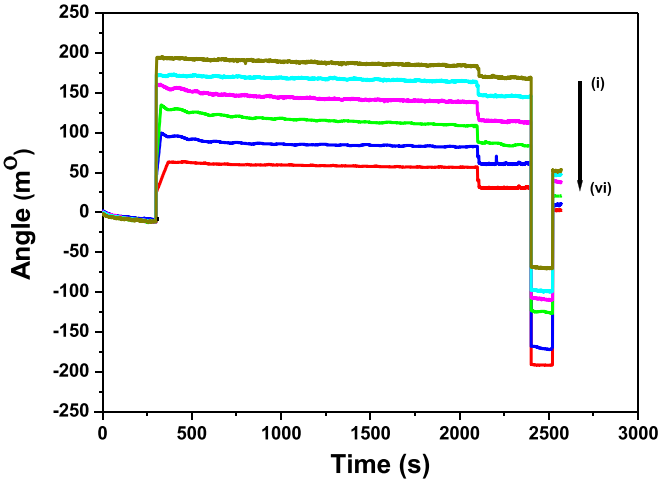

Fig. 4. SPR response of pDNA/CdSe-LB/Au as a function of time for (i) 180 pM, **(ii)** 150 pM, (iii) 110 pM, (iv) 75 pM, (v) 40 pM, and (vi) 5 pM concentrations of complementary DNA.

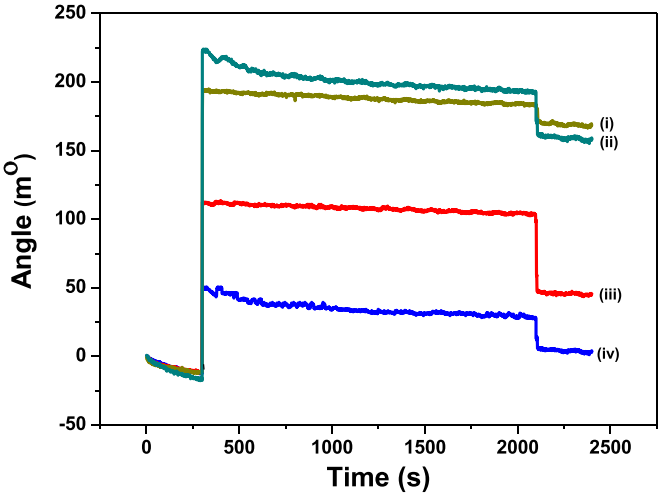

Fig. 5. SPR sensorgrams of pDNA/CdSe-LB/Au for hybridization detection with (i) complementary DNA, (ii) pool of various synthetic DNA sequences, (iii) one-base mismatch DNA and (iv) non-complementary DNA.

complementary sequence (Curve i). The change in θ of about 45 m^0 is seen after hybridization with one-base mismatched sequence (Curve iii) indicating some non-specific binding. However, negligible change (45 m^0) in θ occurs after hybridization with the non-complementary sequence (Curve iv). This observed very small change can be attributed to non-specific adsorption of non-complementary DNA over the pDNA/CdSe-LB/Au disk. The results indicate that the fabricated DNA sensor can be used to discriminate even a single nucleotide variation in target DNA sequence. Attempts have also been made to detect the target complementary DNA sequence among a pool of different DNA sequences. For this purpose, solution containing 180 pM concentration of each of the complementary DNA, non-complementary DNA, one-base mismatch DNA and a few other synthetic DNA sequences was prepared in TE buffer. These DNA sequences were selected in a way that they do not hybridize with each other to form duplex. The solution was then introduced into the channels and the sensor chip was subjected to undergo hybridization and dissociation process. A change in 161 m^0 was obtained after 1800 s (Curve ii), which is comparable to that obtained with sole complementary DNA solution having 180 pM concentration. The results indicate that the sensor could quantitatively detect complementary DNA sequence among the pool of different DNA sequences.

Table 1
Comparison of response characteristics and association constant of fabricated biosensor along with those recently reported in literature for label-free SPR-based hybridization detection.

Sl. No.	Immobilization substrate	Probe modification/signal amplification substance	Detection limit	Test range	Sensitivity	Reference
1	DNA probe/straptavidin/carboxylated dextran/Au	Biotin	0.5 nM	1 μM to 5 nM	435.51 m^0 nM^{-1}	Zhang et al. (2012)
2	DNA probe/Au	Auxiliary probe/biotynalated probe/ streptavidin	9 pM	1 μM to 10 pM	Not mentioned	Ding et al. (2015)
3	DNA probe/Au	Mismatched catalytic hairpin assembly/ streptavidin aptamer	1 pM	100 nM to 5 pM	174.24 m^0 nM^{-1}	Li et al. (2016)
4	DNA probe/AuNP/HDT/Au	AuNp	20 Amol	100 nM to 10 pM	241.0 m^0 M^{-1}	Xiang et al. (2015)
5	Hairpin DNA probe/Au	DNA-linked AuNP/reporter DNA	8 fM	150 pM to 0 pM	Not mentioned	Wang et al. (2016)
6	DNA Probe/CdSe-QD/ODT/Au	CdSe-QD	4.21 pM	180 pM to 5 pM.	0.7859 m^0 pM^{-1}	This work

3.4. Determination of rate constant

Attempts were made to calculate values of the hybridization constant (k_a) and dissociation constant (k_d) for pDNA/CdSe-LB/Au electrode. The kinetic analysis of the hybridization phase was used to obtain the value of hybridization and dissociation rate constants and the equilibrium constant (Ali et al., 2014; Prabhakar et al., 2008). The binding reaction equation for the two macromolecular interactants is given as

$$[A] + [B] = [AB] \quad (1)$$

The rate of formation of complex in hybridization phase is given by:

$$\frac{d[AB]}{dt} = k_a[A][B] - k_d[AB] \quad (2)$$

and k_a and k_d follows relation given by Eq. (3).

$$k_s = k_a[C] + k_d \quad (3)$$

The values of k_s can be obtained by the integrated rate equation for association phase presented in Eq. (4).

$$R_t = E(1 - e^{-k_s t}) + R_0 \quad (4)$$

where

$$E = \frac{k_a C R_{max}}{k_a C + k_d} \quad (5)$$

Here, R_0 represents the signal at zero time, C is the complementary DNA concentration, and E is maximum change in the response. The kinetic information can be obtained from Eq. (3) and calculations have been done by nonlinear curve fitting using kinetic evaluation software. The k_a and k_d are evaluated from the plot of k_s *versus* C where slope of curve gives the value of k_a and intercept yields the information about k_d. The values of k_a and k_d rate constants for complementary DNA hybridization are estimated to be 9.6×10^4 M^{-1} s^{-1} and 2.3×10^{-2} s^{-1}, respectively, with the equilibrium constant for hybridization (k_a/k_d) as 4.2×10^6 M^{-1}. This quantum dot monolayer based SPR biosensor shows higher k_a and k_s values for the complementary target DNA as compared to that obtained using direct immobilization of DNA probe on Au disk (Prabhakar et al., 2008). This shows that application of QD results in improved kinetics of the sensor. Table 1 shows results of these studies along with those reported in literature for SPR-based DNA hybridization sensors. It can be seen that the fabricated sensor presents improved or comparable detection limit and sensitivity as compared to sensors based on streptavidin either employed as a signal enhancing agent or to support the probe DNA immobilization. However, the observed lower detection limit of this sensor as compared to sensors having gold nanoparticles as the signal enhancing agent can be attributed to the localized surface plasmon resonance phenomenon caused by the collective oscillations of surface electrons in noble metal nanoparticles.

4. Conclusions

In the present work, the SPR signal enhancement of Au film has been observed *via* CdSe QD. The QDs are found to excite the surface plasmons to particle plasmons when placed in close proximity to the Au film. The QD monolayer has been deposited over the Au substrate using Langmuir–Blodgett technique that provides organized assembly of QD over the substrate surface. This organized assembly of QD has led to strong optical coupling of incident light to resonance thus enhance the sensitivity (0.7859 m^0 pM^{-1}) of the SPR biosensor. The pDNA/CdSe-LB/Au electrode is found to selectively detect complementary target DNA in the concentration range from 5 pM to 180 pM with a limit of detection as 4.21 pM. The values of hybridization and dissociation rate constants for hybridization event have been found to be 9.6×10^4 M^{-1} s^{-1} and 2.3×10^{-2} s^{-1}, respectively, with the equilibrium constant for hybridization (k_a/k_d) as 4.2×10^6 M^{-1}. The selectivity of the biosensor has been demonstrated by discrimination of single-nucleotide mismatch and non-complementary DNA sequence. The results of these studies clearly demonstrate efficacy of the QD-based SPR sensor as a high throughput device for detecting the specific DNA hybridization. The efforts should be made to utilize this SPR sensor for analysis of clinical samples.

Acknowledgments

We thank Director, NPL, New Delhi, India for the facilities. Financial support received under the Department of Science and Technology project (DST/TSG/ME/2008/18) is gratefully acknowledged.

Appendix A. Supplementary material

Supplementary data associated with this article can be found in the online version at http://dx.doi.org/10.1016/j.bios.2016.02.013.

References

Ali, M.A., Srivastava, S., Pandey, M.K., Agrawal, V.V., John, R., Malhotra, B.D., 2014. Anal. Chem. 86, 1710–1718.

Cennamo, N., Pesavento, M., Lunelli, L., Vanzetti, L., Pederzolli, C., Zeni, L., Pasquardini, L., 2015. Talanta 140, 88–95.
Cheung, J.H., Rubner, M.F., 1994. Thin Solid Films 244, 990–994.
Ding, X., Yan, Y., Li, S., Zhang, Y., Cheng, W., Cheng, Q., Ding, S., 2015. Anal. Chim. Acta 874, 59–65.
Druker, B.J., Sawyers, C.L., Kantarjian, H., Resta, D.J., Reese, S.F., Ford, J.M., Capdeville, R., Talpaz, M., 2001. N. Engl. J. Med. 344, 1038–1042.
Foos, E.E., Wilkinson, J., Mäkinen, A.J., Watkins, N.J., Kafafi, Z.H., Long, J.P., 2006. Chem. Mater. 18, 2886–2894.
Hoa, X.D., Martin, M., Jimenez, A., Beauvais, J., Charette, P., Tabrizian, M., Kirk, A.G., 2007. Lasers and Electro-Optics Society, 2007. In: Proceedings of the 20th Annual Meeting of the IEEE. pp. 598–599.
Huang, H.H., Seeger, C., Helena, D.U., Lindblad, P., 2015. Mol. Biol. BMC Res. Notes, 8.
Ishida, T., Tsuneda, S., Nishida, N., Hara, M., Sasabe, H., Knoll, W., 1997. Langmuir 13, 4638–4643.
Lee, W.I., Kantarjian, H., Glassman, A., Talpaz, M., Lee, M.S., 2002. Ann. Oncol. 13, 781–788.
Li, J., Lei, P., Ding, S., Zhang, Y., Yang, J., Cheng, Q., Yan, Y., 2016. Biosens. Bioelectron. 77, 435–441.
Nawattanapaiboon, K., Kiatpathomchai, W., Santanirand, P., Vongsakulyanon, A., Amarit, R., Somboonkaew, A., Sutapun, B., Srikhirin, T., 2015. Biosens. Bioelectron. 74, 335–340.
Nowell, P.C., 2007. J. Clin. Investig. 117, 2033–2035.
Peng, Z.A., Peng, X., 2000. J. Am. Chem. Soc. 123, 183–184.
Piliarik, M., Párová, L., Homola, J., 2009. Biosens. Bioelectron. 24, 1399–1404.
Prabhakar, N., Matharu, Z., Malhotra, B.D., 2011. Biosens. Bioelectron. 26, 4006–4011.
Prabhakar, N., Arora, K., Arya, S.K., Solanki, P.R., Iwamoto, M., Singh, H., Malhotra, B. D., 2008. Analyst 133, 1587–1592.
Qi, X., Bo, Z., Shan, H., Fangfang, T., Hongliang, G., Yushu, G., Xiaorong, L., Zhike, H., Yi, L., 2009. Nanotechnology 20, 325101.
Saglio, G., Fava, C., 2012. Compr. Cancer Netw. 10, 121–129.
Sharma, A., Pandey, C.M., Matharu, Z., Soni, U., Sapra, S., Sumana, G., Pandey, M.K., Chatterjee, T., Malhotra, B.D., 2012. Anal. Chem. 84, 3082–3089.
Singh, A., Verma, H.N., Arora, K., 2014. Appl. Appl. Biochem. Biotechnol. 175, 1330–1343.
Šípová, H., Homola, J., 2013. Anal. Chim. Acta 773, 9–23.
Tahmasebpour, M., Bahrami, M., Asgari, A., 2015. Opt. – Int. J. Light Electron Opt. 126, 2747–2751.
Tran, D.T., Knez, K., Janssen, K.P., Pollet, J., Spasic, D., Lammertyn, J., 2013. Biosens. Bioelectron. 43, 245–251.
von Holt, B., Kudera, S., Weiss, A., Schrader, T.E., Manna, L., Parak, W.J., Braun, M., 2008. J. Mater. Chem. 18, 2728–2732.
Wang, Q., Liu, R., Yang, X., Wang, K., Zhu, J., He, L., Li, Q., 2016. Sens. Actuators B 223, 613–620.
Xiang, Y., Zhu, X., Huang, Q., Zheng, J., Fu, W., 2015. Biosens. Bioelectron. 66, 512–519.
Zayats, M., Kharitonov, A.B., Pogorelova, S.P., Lioubashevski, O., Katz, E., Willner, I., 2003. J. Am. Chem. Soc. 125, 16006–16014.
Zhang, D., Yan, Y., Li, Q., Yu, T., Cheng, W., Wang, L., Ju, H., Ding, S., 2012. J. Biotechnol. 160, 123–128.